An integrated MILP framework for co-optimizing energy and water systems with up and downward reserve constraints: Application to an off-grid small island

Applied Energy 401 (2025) 126821

Contents lists available at ScienceDirect

Applied Energy

journal homepage: www.elsevier.com/locate/apen

An integrated MILP framework for co-optimizing energy and water systems with up and downward reserve constraints: Application to an off-grid small island

Enrico Giglio [a,b,c,*], Caterina Carà [a,b,c], Edoardo Pasta [a,c], Edoardo Destro [a], Anna Ceni [a,c], Giovanni Bracco [a,c], Giuliana Mattiazzo [a,b,c]

[a] Department of Mechanical and Aerospace Engineering, Politecnico di Torino, Corso Duca degli Abruzzi 24, 10129, Torino, Italy
[b] Energy Center Lab, Politecnico di Torino, Via Paolo Borsellino 38/16, 10138, Torino, Italy
[c] Marine Offshore Renewable Energy Lab (MOREnergy Lab), Politecnico di Torino, Via Paolo Borsellino 38/16, 10138, Torino, Italy

HIGHLIGHTS

- Up/downward reserves increase system cost by 55 % and BESS size by 40 %.
- Energy-water coupling accelerates transition by cutting system costs by 10 %.
- Ignoring operational constraints leads to suboptimal planning outcomes.
- Open-source model tested on a non-interconnected island with water-energy coupling.

GRAPHICAL ABSTRACT

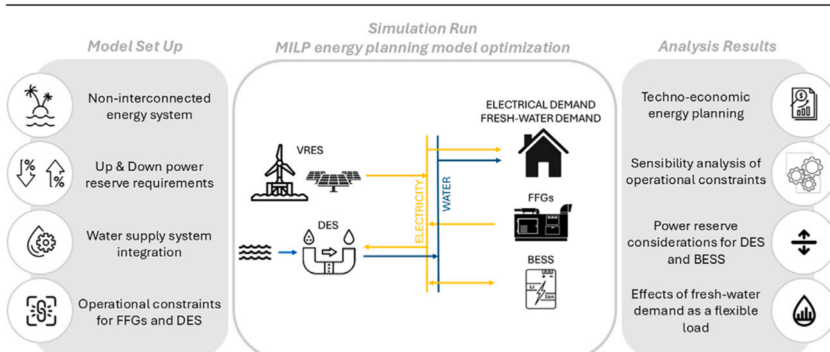

ARTICLE INFO

Keywords:
Energy system modeling
Power reserve requirements
Energy planning
Mixed-integer linear programming (MILP)
PyPSA
Off-grid islands

ABSTRACT

High shares of variable renewable energy sources (vRES) pose growing challenges for power system planning. While these issues are expected to intensify in large-scale systems with increasing vRES deployment, they are already critical in isolated or weakly interconnected areas, where balancing resources are scarce and operational flexibility is limited. Simultaneously, water-intensive infrastructures such as desalinators impose a substantial and often inflexible electricity demand, further stressing system stability. These dual pressures call for a coordinated planning approach that captures energy-water interdependencies while explicitly accounting for reserve adequacy and operational constraints. This study presents an integrated MILP-based framework for co-optimizing energy and water systems. The model incorporates upward and downward reserve requirements and the detailed operational behavior of key technologies, including fuel-fired generators, battery energy storage, and desalination units. Applied to the off-grid island of Pantelleria, the framework quantifies the isolated effects of core features—such as reserve directionality, unit commitment, and flexible desalination scheduling—on system costs, sizing, and dispatch. Results show that explicitly modeling both upward and downward reserves leads to substantially different system configurations, increasing total system costs by up to 55 % compared to scenarios with only upward reserves. Introducing desalination flexibility via load shifting further decreases costs by 10 % while supporting greater vRES penetration. Neglecting these aspects leads to inefficient use of dispatchable assets and

* Corresponding author at: Department of Mechanical and Aerospace Engineering, Politecnico di Torino, Corso Duca degli Abruzzi 24, 10129, Torino, Italy.
Email address: enrico.giglio@polito.it (E. Giglio).

https://doi.org/10.1016/j.apenergy.2025.126821
Received 12 June 2025; Received in revised form 5 September 2025; Accepted 21 September 2025

Available online 6 October 2025

suboptimal planning outcomes. While demonstrated on Pantelleria, the proposed methodology applies broadly to systems where flexibility, sector coupling, and reserve provision are critical. The model is implemented in the open-source PyPSA framework, enabling transparent and extensible energy-water co-planning.

Nomenclature

Acronyms

FFG	Fuel-fired generator
$vRES$	Variable renewable energy sources
$BESS$	Battery energy storage systems
DES	Desalination plants

Indices and sets

g	Indices of fuel-fired generator (FFG) units
r	Indices of vRES generation units
s	Indices of storage units
d	Indices of desalinators
t	Indices of operating snapshots $t = 1, \dots, t_{end}$
n	Indices of nodes
Ω_G	Set of FFGs
Ω_R	Set of vRES generation technologies
Ω_S	Set of storage units
Ω_D	Set of desalinators
Ω_L	Set of loads
Ω_T	Time domain

Parameters

cc	capital costs
oc	operational costs
f_{obj}	objective function
sw_t	weight of the t-th snapshot
sbc_a	standby costs of the a-th component
$f_{ln,t}$	power flow in the ln-th line at t-th time
$K_{ln,n}$	network's incidence matrix in the ln-th line of the n-th node
$\eta^{ch}_{s,n}$	charging efficiency coefficient
$\eta^{dsc}_{s,n}$	discharging efficiency coefficient
η^{sd}_{s}	self-discharge coefficient
$l_{l,n,t}$	mean hourly l-th load
CF_r	capacity factor of r-th vRES unit
$d^{ch}_{s,t}$	mean hourly charge power of the s-th battery
$d^{dsc}_{s,t}$	mean hourly discharge power of the s-th storage unit
e^{max}_{s}	maximum SoC of the s-th storage unit
e^{min}_{s}	minimum SoC of the s-th storage unit
P_a	nominal capacity (power) of the a-th component (FFGs, power converter of s-th storage, vRES techs, desalinators)
E_s	nominal capacity of the s-th storage unit.
$d_{a,t}, d_{a,n,t}$	mean hourly electrical power supplied or procured at t-th time step by the a-th component of the n-th node.
$e_{s,t}$	state-of-charge of the s-th storage at t-th time step.
$d_{w,t}$	mean hourly water produced by all the desalinators at t-th time.
$p^{max}_{a,t}$	maximum percentage of power that can be supplied or procured by the a-th component at t-th time step.
$p^{max}_{s,dsc}$	maximum percentage of safe discharge power of the s-th storage unit
$p^{max}_{s,ch}$	maximum percentage of safe charge power of the s-th storage unit
$p^{min}_{a,t}$	minimum percentage of power that can be supplied or procured by the a-th component at t-th time step.
$s_{a,t}$	status (on/off) of the a-th component at t-th time step
$w_{c,t}$	quantity of water available in the c-th container at t-th time step
$w^{max}_{c,t}$	maximum water capacity coefficient in the c-th container at t-th time step
wd_t	water demand at t-th time step.
d_w	water produced by each d-th desalinator
W_s	water tank maximum available capacity
α_w	stand-by energy consumption coefficient of d-th desalinator.
β_w	specific energy consumption (SEC) per unit of time of each d-th desalinator
T^{d}_{mu}	minimum turn-on time steps
$su_{d,t}$	hourly start-up state of d-th desalinator
$r_{a,t}$	up reserve of the a-th component at t-th time step
$q_{a,t}$	down reserve of the a-th component at t-th time step
R^{rq}_{t}	up reserve requirement
Q^{rq}_{t}	down reserve requirement
ε_r	percentage of power reserve demand w.r.t. total mean hourly available vRES
ε_l	percentage of power reserve required w.r.t. total mean electrical load
ε_{fix}	fixed term of the hourly reserve request

1. Introduction

The global energy landscape is increasingly dominated by renewable energy sources (RES), with variable RES (vRES) playing a growing role in electricity generation [1]. While this transition is critical for reducing carbon emissions, the variability and unpredictability of vRES pose significant challenges for maintaining power system stability, especially at high vRES penetration levels [2]. Effective planning strategies that incorporate both upward and downward reserve requirements are essential to manage these fluctuations and maintain high levels of vRES integration [3].

This issue is particularly pronounced on islands and remote regions that are disconnected from the mainland grid [3,4]. These areas typically rely on polluting fuel-fired generators (FFGs) for electricity, which often operate inefficiently when required to provide back-up capacity [5]. In addition, many islands rely heavily on desalination plants (DES), which contribute significantly to overall electricity consumption [6], adding to the complexity of RES integration and reserve management [7]. As desalination accounts for a large proportion of energy demand, any planning process must take into account its impact on the operation of the power system [8]. In addition to addressing the challenges posed by FFGs inefficiencies and desalination loads, it is critical to model the role of battery energy storage systems (BESS) in providing reserve capacity [9]. BESS can increase system flexibility by absorbing excess power, and releasing it during periods of low supply, effectively balancing fluctuations in supply and demand [10]. Incorporating BESS into planning strategies is essential to ensure a stable energy transition, as they can help meet reserve requirements more efficiently than traditional generation units [11].

1.1. Paper positioning

Numerous studies have extensively modeled the operating characteristics of FFGs, i.e., considering start-up costs, ramp rates and minimum up/down times [12–14]. However, these works often neglect downward reserve requirements and focus exclusively on upward reserve provision. This limitation can lead to non-optimal planning results, as downward reserves are critical for managing and ensuring system stability under varying load and vRES generation conditions.

Other studies address both upward and downward reserve requirements, recognizing their combined importance in maintaining system stability, especially under high renewable penetration [15,16]. However, these studies often provide limited operational FFGs characterization (i.e., stand-by cost), thus neglecting its critical impacts. They also fail to consider the integration of energy-intensive water systems, treating total electricity demand as a static input and overlooking potential synergies between energy and water systems. Few studies consider both upward and downward reserves and operational constraints, but often optimize over limited time horizons, which may not capture the full operational dynamics of isolated energy systems [17].

Several studies investigate the role of BESS in providing reserve capacity [18], often alongside detailed operational modeling of FFGs [19]. Regardless of the reserve type—upward, downward, or both—BESS consistently provide reserves efficiently, thanks to their ability to quickly switch between charging and discharging [20]. This underscores the importance of integrating BESS into energy planning to reduce reliance on conventional generators and enhance system flexibility and stability.

Moving on to the integration of water systems into energy planning, a subset of the literature focuses primarily on the operational characteristics of DES, detailing their energy consumption patterns, operational constraints, and impact on meeting water demand, often providing valuable insights into the efficiency and reliability of individual desalination systems [21,22]. However, they fail to consider how these energy-intensive systems interact with the broader energy infrastructure or their potential role as reserve providers, isolating desalination operations from overall energy planning and overlooking their capacity to support grid stability by adjusting water production in response to fluctuations in energy supply and demand [4,23]. Other studies recognize the potential of DES as flexible loads that can contribute to the provision of reserves, in particular by adjusting water production schedules to match grid requirements [24]. While this highlights the role of water systems in supporting grid stability, these works tend to focus narrowly on reserve provision without addressing their integration into the broader energy planning framework [25]. Nevertheless, these studies overlook the potential benefits of integrating water systems into energy planning, neglecting sector-coupling synergies and resulting in non-optimal resource use, limited vRES integration, and higher overall system costs.

These gaps motivate the development of a comprehensive modeling framework that explicitly integrates reserve requirements, realistic operational constraints, and sector coupling aspects—laying the foundation for the methodological approach presented in this work.

1.2. Contributions

In response to the research gaps discussed in Section 1.1, this study proposes a comprehensive modeling framework for integrated energy-water system planning, which incorporates upward and downward reserve requirements alongside the operational constraints of key technologies such as FFGs, BESS, and DES. The framework is designed to support cost-effective and resilient energy transitions, especially in systems characterized by limited flexibility, high vRES penetration, and strong water-energy interdependencies. In addition to proposing an all-encompassing modeling framework to enhance energy-water co-planning under reserve and operational constraints, this study contributes to the following specific areas:

- A comparative and critical review of the literature on reserve requirements and desalination integration in energy planning, highlighting existing methodological gaps and motivating the development of a more integrated and operationally detailed modeling framework;
- Introduction and assessment of key modeling features—namely upward reserve, downward reserve, flexible desalination scheduling, and unit commitment constraints—through a structured step-by-step approach. Each feature is progressively introduced and its isolated impact on system planning outcomes is quantified, enabling a detailed understanding of its role in supporting energy-water co-optimization;
- Particular attention is given to the evaluation of freshwater demand as a flexible load within the energy system, demonstrating how optimized desalination scheduling can reduce BESS capacity requirements, improve vRES integration, and lower overall system costs without affecting total water supply;
- Integration of the proposed model within the open-source PyPSA energy modeling framework, demonstrating its extensibility to include water sector components, and enabling further development and adaptation by the research community.

The framework is validated through an application to the island of Pantelleria, a non-interconnected Mediterranean system characterized by high RES potential, limited operational flexibility, and energy-intensive water demand. While the case study positions this work as a benchmark for planning in off-grid and weakly interconnected contexts, the proposed methodology is broadly applicable to any system where reserve adequacy, sector coupling, and flexibility constraints are critical.

1.3. Structure of the work

The paper opens with a review of recent contributions on reserve requirements and desalination integration in energy planning, providing the necessary background for the proposed modeling framework. The integrated energy-water planning formulation, based on an MILP structure that captures both electricity and water sector dynamics, is then presented in Sections 3 and 4 which introduces the case study of the non-interconnected island of Pantelleria, together with the scenario definition approach and the computational setup adopted for simulations. Finally, Section 5 discusses the simulation results and evaluates the impact of the key modeling features on system performance.

2. Integrated water-energy planning approaches for isolated systems: state-of-the-art

Numerous studies have investigated optimal planning and operational strategies for stand-alone power systems, typically based on conventional generation [26]. While these works have emphasized the role of storage and vRES in supporting decarbonization goals, they often overlook the broader technical implications of transitioning to high-RES systems [27,28]. In particular, developing models that are both computationally efficient and technologically comprehensive remains an open challenge—especially in contexts requiring detailed operational constraints and integrated sector planning [3].

One of the core issues in non-interconnected systems is the growing instability resulting from the intermittency and unpredictability of vRES, which often leads to supply-demand imbalances [29]. To address this major concern and try to cope with it, studies have proposed methodologies taking into account the power reserve capacity necessity, which indeed must always be available for real-time balancing [30]. In general, power reserves are commonly classified along two complementary dimensions. The first refers to their response time [31,32]: typically *primary* when the response can be quantified in seconds, *secondary* when the response spans from seconds to minutes, and *tertiary* when it requires from minutes up to hours. The second classification considers the direction of activation [33]: *upward* reserves are activated to meet an unexpected increase in demand or a generation failure in the power system, while *downward* reserves are used to cope with excess generation or sudden drops in load.

Among the examples of studies that try to include reserve considerations in the optimal operation and planning, Hansen et al. [34] modeled the optimal dispatching for the island of Crete, roughly considering the operational characteristics of the FFGs—only the initial start-up costs—and taking into account only primary, secondary and tertiary upward reserves provided by conventional diesel and gas turbines, highlighting the importance of the storage system to avoid high wind curtailment during periods of high wind resource availability and low electricity load. Similarly, Nikolaidis et al. [35] focused on minimizing the upward spinning reserve requirements for the island of Cyprus, modeling thermal units with a high level of operational and technical detail, as well as incorporating BESS. However, despite this detailed approach, the study does not take downward reserves into account. Finally, for the island of Pantelleria, Giglio et al. [36] modeled the upward reserve requirements, analyzing FFGs along with vRES and BESS as potential reserve providers. Despite the key findings on the critical role of BESS and the limited impact of vRES in reserve provision, the study does not take into account downward reserves.

Some studies have expanded the analysis to include downward reserve requirements, recognizing their role in ensuring operational stability in systems with high vRES penetration. This is particularly relevant for FFGs in small off-grid systems, which often operate close to their minimum technical output, limiting their ability to absorb fluctuations caused by sudden drops in demand or surges in vRES [37]. Without explicit modeling of downward reserves, optimization strategies may fail to capture these dynamics, leading to limited vRES integration and suboptimal use of storage and generation assets. In this context, Psarros et al. [17] presented a unit commitment economic dispatch model that considers reserve requirements at different timescales (primary up/down, secondary up/down and tertiary spinning reserves), but only the reserve capability of the generating units is considered to address the phenomenon of grid unpredictability. Another interesting contribution is provided by Critz et al. [38] and De Vos et al. [30], who both considered the issue of up/down spinning reserves to support vRES integration on the islands of Hawaii and Cyprus, respectively. The former analyzed the effectiveness of demand-response mechanisms in smoothing system operations, while the latter focused on the need to update reserve policies to accommodate the unavoidable increase in vRES penetration for decarbonization and to avoid demand shedding. Nevertheless, both studies only consider FFGs as reserve providers and apply limited operational constraints in their characterization. Groppi et al. [15] performed a long-term optimization of the Favignana island power system focused on the diversification of technology providing reserves, highlighting the key role of biomass, BESS, gas generators, hydrogen and also electric boilers, considering both upward and downward reserve requirements, but with a limited characterization of FFGs operational features -only ramp up/down, and minimum/maximum power. Both Psarros et al. [39] and Curto et al. [16] studied the reserve concept respectively for small non interconnected islands, taking into account also the role of the BESS. However, the former focused on the minimization of the vRES curtailment for a more efficient operation of thermal units; the latter operated to reduce the use of FFGs providing synthetic inertia by means of the BESS.

In addition to the limited technological diversification for reserve provision, a key shortcoming of most studies is the static treatment of electricity demand. This assumption overlooks the flexibility potential of energy-intensive processes such as desalination, which could support power system balancing through load shifting. Several contributions have addressed this aspect by explicitly modeling water demand and its impact on energy planning, highlighting the role of desalination as a flexible load that can improve system efficiency and enable greater vRES integration [40]. Indeed, the energy landscape can be better characterized by adopting a comprehensive energy system approach that specifically models the water load alongside the technical components of the system. This approach positions water demand as a key player in load shifting, which has the potential to reduce the size of BESS and accelerate the decarbonization process. By increasing the flexibility of the grid, this integration enables a higher penetration of vRES. Mentis et al. [21] combined the DES of the Aegean islands with the vRES-based power system, focusing on the decarbonization of their energy demand. Oikonomou et al. [41] analyzed the role of DES in frequency regulation and demand response, showing how they can participate in both upward and downward reserve provision. Furthermore, Corsini et al. [25] modeled the water system and its different components, considering the role of DES as a renewable energy buffer compared to the hydrogen vector. Segurado et al. [23] analyzed the energy system of S. Vicente Island in Cape Verde, modeling the energy system while considering the water tank levels directly related to the water demand supply and the electricity demand related to the plant. Groppi et al. [42] proposed a long-term energy planning framework for Favignana Island, integrating the energy and water systems with hourly resolution. Their analysis aims to evaluate optimization outcomes under various policy approaches for emission containment, emphasizing the importance of considering both local water production and imports. However, the study does not account for the operational characteristics of the DES or the differing features of the power system. Finally, Kavei et al. [43] analyzed the water-energy nexus on Pantelleria Island using the TEMOA framework, integrating the Reference Water System and Reference Energy System. The study highlights the impact of water reuse and improved distribution networks on energy demand in fragile island systems. However, the model lacks operational constraints, such as unit commitment for FFGs and desalination system features, as well as reserve requirements and grid stability, limiting its applicability for small, isolated grids. These gaps highlight the need for future enhancements to include more robust operational modeling, ensuring that the proposed solutions align with the practical challenges of integrating water and energy systems.

Although these studies recognize the energy-intensive components of island energy systems, their modeling efforts in terms of energy system configuration and operational characteristics fail to simultaneously consider all the key actors present. This oversight limits their ability to accurately characterize the system and provide reliable solutions for decarbonization and management, especially when considering relevant technical constraints such as the operational characterization of FFGs, the diversification of energy-intensive island demand (including electricity and water), reserve requirements for power system stabilization, the penetration of vRES and the role of storage.

Table 1 presents a comparison of the aforementioned studies, summarizing their key features and highlighting the associated gaps. While many papers address specific aspects of the problem, this study contributes, to the best of the authors' knowledge, by jointly optimizing energy mix planning and operational configuration for island systems, addressing both electricity and water demand. In addition, it incorporates power system operational constraints and accounts for the role of multiple technologies in flexibility management. The modeling framework presented in the next section is developed in direct response to these gaps, aiming to provide a comprehensive tool for integrated planning in isolated energy-water systems. Fig. 1 illustrates the structure of the proposed framework, summarizing the main input data, optimization layers and output metrics across both the energy and water domains.

3. The proposed comprehensive MILP energy planning model

The MILP planning problem is set in the PyPSA framework [44], which operates with the goal of minimizing a cost objective function detailed in the following section. Equations to model the electrical balance between generation and consumption among the different nodes are described in Section 3.2. Constraints to ensure the stability of the power system by fulfilling the power reserve requirements are presented in Section 3.4 and 3.5.

Table 1
Comparison of relevant studies on energy planning for non-interconnected systems, highlighting modeled reserve types, technology roles, demand characterization, and operational constraints.

Ref	reserve considerd		type of technologies as reserve					Type of demand		Applied constraints on operationals of FFGs
	up	down	FFG	vRES	Storage	Desalination plant	others	electricity	water	
[34]	X		X	X				X		start up cost
[35]	X		X		X			X		start up, shut down cost,minimum up and down time after start up ot shut down; ramp up ramp down
[36]	X		X	X	X			X		idling costs, committability, min rate power
[17]	X	X	X					X		start up costs (cold, warm, hot), shutdown cost, remuneration of the provided active power reserve. Start-up costs for each unit, shut down costs, constrainint the max number of startup operations over the time horizon
[38]	X	X	X					X		
[30]	X	X	X					X		fuel cost, co2 emissions costs, start up cost, max and min output level, ramp rate min up and down time
[15]	X	X	X	X	X		electrolyser, biomass, electric boilers	X		ramp up, ramp down, pmin, pmax
[39]	X	X	X		X			X		start up, shut down, status/ commitment, (no ramp), p min, p max
[16]	X	X	X		X			X		
[21]								X	X	
[41]	X	X				X		X	X	
[25]								X	X	
[23]								X	X	
[42]								X	X	
[43]								X	X	
This work	X	X	X		X	X	X	X	X	

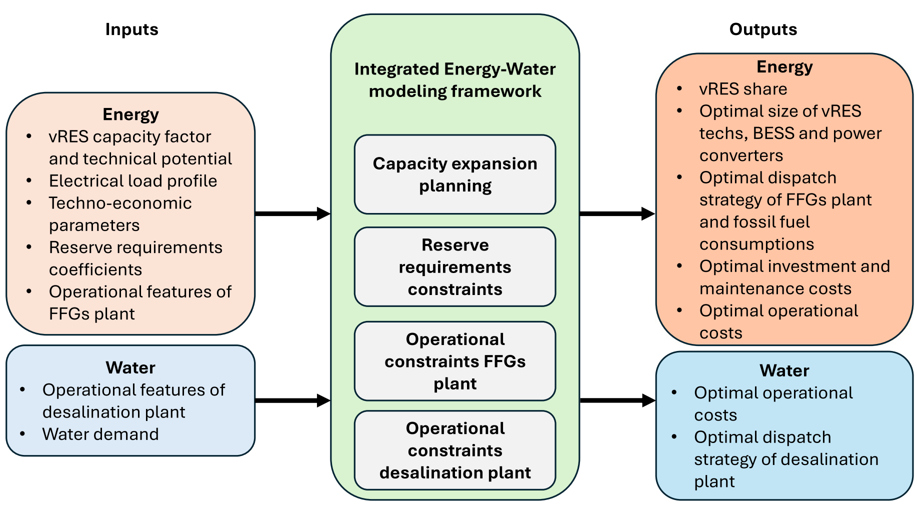

Fig. 1. Schematic overview of the integrated energy-water modeling framework, showing main inputs, MILP optimization layers, and key outputs on system configuration, dispatch, and costs.

3.1. Objective function

The techno-economic optimization of the MILP problem is performed with the objective of minimizing the Net Present Cost (NPC) of the power system, as outlined in Eq. (1). The formulation of the optimization accounts for the total annualized capital costs (CC_{tot}), the total operational costs (OC_{tot}), and the weight of the t-th snapshot (sw_t).

$$\min f_{obj}^{base} = \min \left\{ CC_{tot} + OC_{tot} \right\} \tag{1}$$

In Eq. (1), the total annualized capital costs CC_{tot} are defined as:

$$CC_{tot} = \sum_{g=1}^{\Omega_G} cc_g \cdot P_g + \sum_{r=1}^{\Omega_R} cc_r \cdot P_r + \tag{2}$$

$$+ \sum_{s=1}^{\Omega_S} \left(cc_s \cdot E_s + cc_{s,links} \cdot P_s \right), \tag{3}$$

where P_g represents the optimal capacity of the g-th FFG, multiplied by its specific capital cost cc_g. Similarly, P_r and E_s are the optimal capacities for vRES techs and storage units, multiplied by their respective capital costs cc_r and cc_s. The term $cc_{s,links} \cdot P_s$ accounts for the capital cost of the power converter associated with the storage units. The total operational costs, OC_{tot} employed in Eq. (1), are defined as:

$$OC_{tot} = \sum_{t=1}^{t_{end}} sw_t \cdot \left(\sum_{g=1}^{\Omega_G} oc_g \cdot d_{g,t} + \sum_{g=1}^{\Omega_G} sbc_g \cdot s_{g,t} + \sum_{s=1}^{\Omega_S} oc_s \cdot d_{s,t} + \sum_{d=1}^{\Omega_D} sbc_d \cdot s_{d,t} \right) \tag{4}$$

where the term oc_g represents the specific operational cost per unit of energy for the g-th generator, while $d_{g,t}$ is the mean power delivered by this generator during the t-th time step. Similarly, oc_s denotes the operational cost for storage units, calculated based on the mean power $d_{s,t}$ provided by the s-th storage unit. The standby costs, sbc_g, reflect the expenses associated with keeping the g-th generator online when it is not actively producing energy, with $s_{g,t}$ indicating its operational status (on/off). Additionally, the stand-by costs associated with the DES are taken into account, sbc_d, covering the expenses of the operators running the facility, combined with the operational status of the plant $s_{d,t}$.

3.2. Electric balance constraints

The electric balance at each node $n \in \Omega_N$ is ensured by Eq. (5), where $f_{ln,t}$ is the power flow in the ln-th line with the network's incident matrix $K_{ln,n}$, and $\eta^{ch}_{s,n}$ and $\eta^{dsc}_{s,n}$ are the charging and discharging efficiency coefficients, respectively. Eqs. (6)–(11) ensure that the power generated by the generators and storage power converters, as well as the energy stored in accumulators, always remains within maximum capacity and technical minimum limits, also considering the possibility for components to be turned off through the status variable $s_a(t)$. Finally, Eq. (12) ensures the balance for each storage unit across different time steps, including the self-discharge coefficient η^{sd}_s.

$$\sum_{a \in (\Omega_G \cup \Omega_R)} d_{a,n,t} + \sum_{s \in \Omega_S} d^{dsc}_{s,n,t} \cdot \eta^{dsc}_{s,n} + \sum_{ln \in \Omega_{LN}} f_{ln,t} \cdot K_{ln,n} = \sum_{s \in \Omega_S} \frac{d^{ch}_{s,n,t}}{\eta^{ch}_{s,n}} + \sum_{l \in \Omega_L} l_{l,n,t} + \sum_{d \in \Omega_D} d_{d,n,t} \tag{5}$$

$$d_{a,t} \le s_{a,t} \cdot P_a \cdot p^{max}_{a,t}, \quad a \in \Omega_G \cup \Omega_S \cup \Omega_R \tag{6}$$

$$e_{s,t} \le E_s \cdot e^{max}_s, \quad s \in \Omega_S \tag{7}$$

$$e_{s,t} \ge E_s \cdot e^{min}_s, \quad s \in \Omega_S \tag{8}$$

$$d_{a,t} \ge s_{a,t} \cdot P_a \cdot p^{min}_{a,t}, \quad a \in \Omega_G \cup \Omega_S \cup \Omega_R \tag{9}$$

$$s_{a,t} = \begin{cases} 1 & \text{if a-th component online} \\ 0 & else \end{cases} \tag{10}$$

$$d_{r,t} \le P_r \cdot CF_{r,t}, \quad r \in \Omega_R \tag{11}$$

$$e_{s,t} = e_{s,t-1} \cdot (1 - \eta^{sd}_s) - d^{dsc}_{s,t} + d^{ch}_{s,t} \cdot \eta^{ch}_s, \quad s \in \Omega_S \tag{12}$$

3.3. Integration of the water system

Eq. (13) models the total d_w water produced by each d-th desalinator. α^d_w is the stand-by energy consumption coefficient, while β^d_w is the specific energy consumption (SEC) per unit of time of each desalinator. Eq. (14) guarantees that the water in the tank ($w_{c,t}$) does not exceed the maximum available capacity, while Eq. (15) guarantees the fulfillment of the water demand wd_t at each time step t-th. Eqs. (16) and (17) ensure that the power consumed by the d-th desalinator is limited by the operating conditions defined by the status of the desalinator and the percentage maximum and minimum working load.

$$d_{d,t} = \sum_{d \in \Omega_D} \alpha_w \cdot s_{d,t} + d^d_{w,t} \cdot \Delta t \cdot \beta_w \tag{13}$$

$$w_{c,t} \le W_s \cdot w^{max}_{c,t}, \quad \forall t \in \Omega_T \tag{14}$$

$$w_{c,t} = w_{c,t-1} - wd_t + \sum_{d \in \Omega_D} d^d_{w,t} \tag{15}$$

$$d_{d,t} \le s_{d,t} \cdot P_d \cdot p^{max}_{d,t}, \quad d \in \Omega_D \tag{16}$$

$$d_{d,t} \ge s_{d,t} \cdot P_d \cdot p^{min}_{d,t}, \quad d \in \Omega_D \tag{17}$$

In Eq. (18), the variable representing the start-up of each d-th desalinator is defined as a binary variable. Specifically, Eqs. (19) and (20) ensure that once the d-th desalinator is activated, it remains operational for a minimum duration of T^d_{mu} time steps, in accordance with the correct operational behavior described in [45].

$$su_{d,t} = \begin{cases} 1 & \text{if d-th desalinator starts-up} \\ 0 & else \end{cases} \tag{18}$$

$$su_{d,t} \ge s_{d,t} - s_{d,t-1}, \quad d \in \Omega_D \tag{19}$$

$$\sum_{t'=t}^{t+T^d_{mu}} s_{d,t'} \ge su_{d,t} \cdot T^d_{mu}, \quad d \in \Omega_D \tag{20}$$

3.4. FFGs contribution to power reserve

Eqs. (21) and (22) model the contribution of FFGs to up- and downward power reserves, accounting for the states of the generators.

$$r_{g,t} \le P_g \cdot s_{g,t} \cdot p^{max}_{g,t} - d_{g,t}, \quad g \in \Omega_G \tag{21}$$

$$q_{g,t} \le d_{g,t} - P_g \cdot s_{g,t} \cdot p^{min}_{g,t}, \quad g \in \Omega_G \tag{22}$$

3.5. BESS contribution to power reserve

Eqs. (23) and (26) model the contribution of BESS to the fulfillment of the up- and downward power reserves. The proposed model implicitly assumes that BESS can switch from charge to discharge (and vice versa) in a time that does not affect the response times required for power reserve.

$$r_{s,t} \le \eta^{dsc}_s \cdot (P_s \cdot p^{max}_{s,dsc} - d^{dsc}_{s,t}) + d^{ch}_{s,t} \tag{23}$$

$$r_{s,t} \le \eta^{dsc}_s \cdot (e_{s,t} - E_s \cdot e^{min}_{s,t}) + d^{ch}_{s,t} \tag{24}$$

$$q_{s,t} \le P_s \cdot p^{max}_{s,ch} - d^{ch}_{s,t} + d^{dsc}_{s,t} \cdot \eta^{dsc}_s \tag{25}$$

$$q_{s,t} \le \frac{E_s \cdot e^{max}_{s,t} - e_{s,t}}{\eta^{ch}_s} + d^{dsc}_{s,t} \cdot \eta^{dsc}_s \tag{26}$$

3.6. Water desalinator contribution to power reserve

Eqs. (27) and (29) model the contribution of DES to the fulfillment of the up- and downward power reserves. Eq. (29) shows how the contribution of the desalinator to the power reserve is also limited by the available capacity in the freshwater storage tank.

$$r_{d,t} \leq d_{d,t} - P_d \cdot s_{d,t} \cdot p_{d,t}^{min} \tag{27}$$

$$q_{d,t} \leq P_d \cdot s_{d,t} \cdot p_{d,t}^{max} - d_{d,t} \tag{28}$$

$$\sum_{d \in \Omega_D} q_{d,t} \leq \frac{W_s \cdot w_{c,t}^{max} - w_{c,t} - \alpha_w}{\beta_w} \tag{29}$$

3.7. Power reserve requirements

Eqs. (30) and (33) model the up- and downward power reserve requirements for each time step t-th. According to the approach adopted in [36], the demand for the power reserve is assumed to be proportional to the power available from vRES and the loads, plus a fixed term.

$$\sum_{a \in \Omega_G \cup \Omega_S \cup \Omega_D} r_{a,t} \geq R_t^{rq} \tag{30}$$

$$\sum_{a \in \Omega_G \cup \Omega_S \cup \Omega_D} q_{a,t} \geq Q_t^{rq} \tag{31}$$

$$R_t^{rq} = \epsilon_r^{up} \cdot \sum_{r \in \Omega_R} (CF_{r,t} \cdot P_r) + \epsilon_l^{up} \cdot \sum_{l \in \Omega_L} l_{l,t} + \epsilon_{fix}^{up} \tag{32}$$

$$Q_t^{rq} = \epsilon_r^{dw} \cdot \sum_{r \in \Omega_R} (CF_{r,t} \cdot P_r) + \epsilon_l^{dw} \cdot \sum_{l \in \Omega_L} l_{l,t} + \epsilon_{fix}^{dw} \tag{33}$$

4. Case study and simulation settings

Pantelleria, a small island with a permanent population of 7700, experiences substantial tourist influxes during the summer months. Due to its isolation from the mainland electricity grid and its rich solar and wind potential, the island is an ideal candidate for examining energy self-sufficiency through a micro-grid-based energy planning model.

The energy system modeled in this study consists of Lithium-ion BESS, Photovoltaic (PV) panels, Floating Offshore Wind Turbines (FOWT), and FFGs (see Fig. 2). The FFGs, which serve as the island's current primary energy source, have a total installed capacity of 26 MW, distributed across eight units: five generators of 4 MW each and three of 2 MW each [36]. The island's electricity demand reached approximately 37 GWh in 2019, with a peak load of 9.5 MW and a base load of 2.2 MW [36].

Offshore wind resources benefit from an average capacity factor of 40 %, while solar resources reach about 19 %. However, PV capacity is capped at 15 MW and onshore wind is excluded due to local restrictions on onshore installations [46]. The investment and operating costs for these technologies are detailed in Table 2, and a 5 % discount rate is applied throughout the analysis [36]. The percentage coefficients relating to the up and down reserve requirements are set at 10 %, with the fixed reserve requirements assumed to be 1.1 MW (the size of the minimum installed diesel generator) [36].

Regarding the BESS system, a round-trip efficiency of 90 % is considered, equally divided between charging and discharging, with a C-rate ranging from 1 to 0.5. The assumed BESS degradation cost is 3 cents €/kWh, based on a projected lifetime of 10,000 cycles. The State of Charge (SoC) is balanced across all simulations, ensuring the initial and final SoC levels are equal.

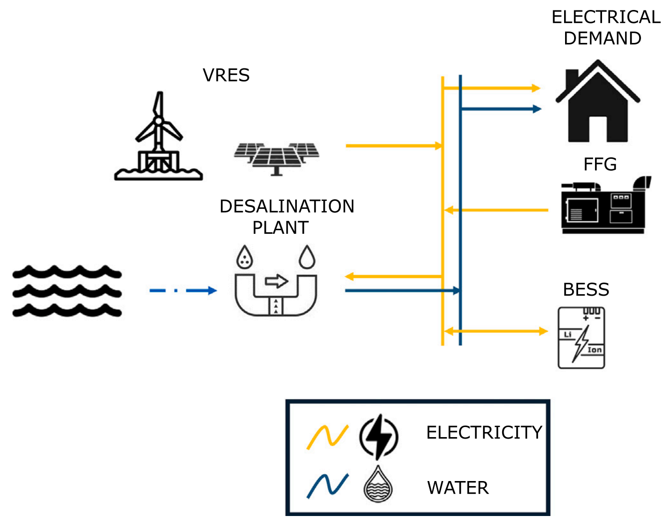

Fig. 2. Scheme of the optimized Water-Energy system.

Table 2
Cost assumptions related to RES technologies, based on [36].

Technology	CapEx	OpEx	Op. Lifetime	Marginal	Stand-by cost
PV	905 $\frac{€}{kWh}$	17 $\frac{€}{kW \cdot y}$	25 years	–	–
FOWT	4500 $\frac{€}{kWh}$	94 $\frac{€}{kW \cdot y}$	25 years	–	–
Li-ES	300 $\frac{€}{kWh}$	6 $\frac{€}{kW \cdot y}$	15 years	–	–
Power converter	180 $\frac{€}{kW}$	18 $\frac{€}{kW \cdot y}$	15 years		
Diesel generators	–	–	–	426 $\frac{€}{MWh}$	69 $\frac{€}{h \cdot MW}$
Desalination plant	–	–	–	–	25 $\frac{€}{h}$ 50 $\frac{€}{h}$ 37.5 $\frac{€}{h}$

The DES has an installed capacity of 1 MW, with a minimum operational load of 10 % and a minimum up-time of 3 h [45,47]. Freshwater demand, which is modeled considering the electricity demand distribution [21], reaches an annual total of $1.08 \cdot 10^6$ m^3, with peak hourly consumption of 350 m^3 occurring during the summer months, and minimum demand of 60 m^3 during off-peak periods. α is neglected and β is $4.5 \frac{kW}{m^3}$ [48,49]. The stand-by costs associated with the DES sbc_d are equal to 25 $\frac{€}{h}$ during morning and afternoon working hours during the workweek (8:00 a.m.–7:00 p.m.), it doubles during overnight hours during the workweek (8:00 p.m.–7:00 a.m.), and it increases by 50 % for morning and afternoon working hours during weekend.

Simulation tasks were executed using the Gurobi solver (version 11.0) on an AMD Ryzen 9 3900X processor with 128 GB of RAM.

4.1. Procedure for the scenario selection

The objective of this paper is to evaluate the operational impacts of three key aspects on energy planning in an isolated power system: (1) up and down reserve requirements, (2) water system integration in a MILP energy planning model, and (3) the operation of FFGs and DESs. Simulations, as reported in Table A.3, were structured step-by-step to assess both individual and combined effects, as outlined below:

1. **Reserve requirements**: Simulations tested up, down, and combined up and down reserves, considering different technologies capable of providing these reserves (FFGs, FFGs + BESS, and FFGs + BESS + DESs).

2. **FFG operational impact**: Focused on the role of stand-by costs, assessing their influence on system performance and their impact on vRES technology energy planning.
3. **DES operational impact**: Analyzed the minimum working load, stand-by costs, and minimum up-time requirements for DES, as well as their impact on system performance and vRES technology energy planning.
4. **Water system integration**: In scenarios where water system integration was removed, desalination demand was added directly to the electricity load, thereby eliminating the optimizer's ability to schedule water production flexibly.

All scenarios were simulated for 9 typical weeks (TW), 63 representative days, with an hourly resolution. A subset of scenarios was also simulated for a full year (FY) to validate the results. Typical weeks were selected through direct sampling of representative days based on average daily profiles of electrical load and renewable availability, without applying clustering or statistical reduction algorithms. While simple, this method is widely adopted in the literature and ensures transparency and reproducibility [50,51], especially when computational scalability is a concern. Gap tolerances were maintained below 2 % to ensure accuracy. However, in scenario FF-UF—where only FFGs provide reserves and only up-power reserve requirements are integrated into the MILP energy planning problem, along with all the operational features of both FFGs and DESs—the solver did not converge within 100 hours. For this scenario, the MIPGap was increased to 3 %.

5. Results and discussions

All scenarios presented in Table A.3 were solved with constraints on MIPGap and the time horizon as explained in Section 4.1. The results, shown in Table B.4, are presented in detail and discussed in the following sections.

5.1. Comparison of full year vs. typical days optimizations

The scenarios proposed in Table A.3 are computationally intensive, necessitating an approach that simulates hourly profiles over 9 TW rather than the entire year. Before applying this approach to all scenarios, selected scenarios were simulated across all hours of the FY and then compared to the results obtained using the typical week simulations. Scenarios were chosen to represent different reserve requirements (only up, only down, and both up- and downward power reserve), covering the broadest range of reserve provision cases (where all technologies—FFGs, BESS, and DES—can supply reserves). Additionally, a scenario was included in which the water load was fixed as part of the electric load, rather than optimized.

Fig. 3 compares the optimal nominal capacities for FOWT and BESS across the different MILP energy planning scenarios (PV capacity was consistently saturated at 15 MW). The figure also shows the annualized system cost, which corresponds to the objective function. The results show that moving from FY to TW simulation slightly affects the optimal sizing side, where the sizing of the technologies varies between 0 % and 10 % across the different scenarios simulated, except for the BESS in the only up reserve scenario UFBW. Considering the objective function, the variation between FY and TW is between 10 % and 15 %. This level of accuracy is acceptable for this study. Consequently, the detailed analysis will proceed using the TW approach as the time horizon for simulations.

5.2. Reserve modeling settings impact on energy planning

The goal of this section is to analyze the impact of different reserve modeling settings on the MILP energy optimization. This includes both the modeling of power reserve requirements and the configuration of technologies that can provide these reserves. To isolate the effects of reserve settings, scenarios were selected where all operational features of FFGs and DESs are consistently applied, ensuring that reserve settings are the only variable factors across scenarios.

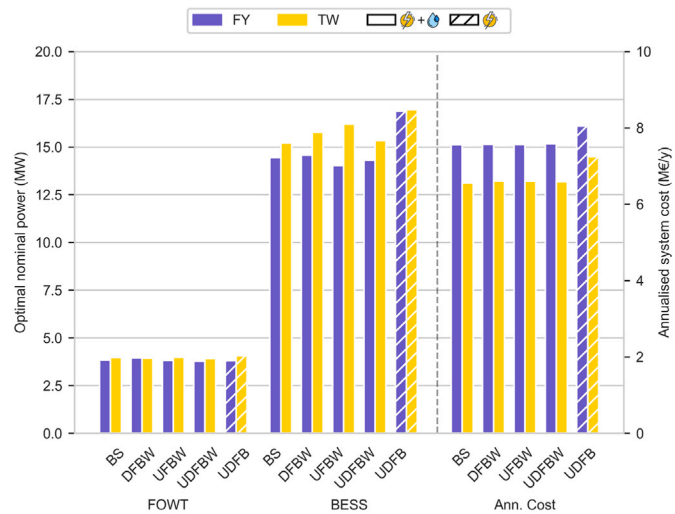

Fig. 3. Technology sizing and costs.

Fig. 4 illustrates the optimal capacity planning for the main power system components (PV, FOWT, and BESS), as well as the annualized system cost, annualized operational cost for DES, and specific operational cost for FFGs. Rather than presenting absolute values, the figure displays the percentage variations of each scenario relative to the base scenario (BS), where no reserve requirements are integrated. Notably, one of the scenarios excludes the water desalination system, preventing the model from optimizing freshwater production independently. Detailed evaluations on the integration of water production are discussed in a dedicated section, but it is worth noting that, in this case, no operational costs are shown for DES since the desalination system is not integrated into the MILP energy model. The figure highlights that, when only FFGs are used to meet reserve requirements, neglecting reserve constraints entirely (as in the BS) leads to a significant overestimation of PV, BESS, and FOWT capacities. Specifically, results show a huge difference for the up- and downward reserve scenario typology, where FOWT, BESS and PV optimal sizing differ from the BS by around the 50 % for the former, to the 60 % for the latter two. Only down reserve scenario has a maximum percentage variation of around 55 % for the FOWT, while the only up reserve scenario has a maximum variation of around 6 %.

In scenarios where only FFGs provide reserves, modeling constraints for only upward reserve requirements result in substantial overestimation of PV, FOWT, and BESS capacities compared to scenarios with only downward reserve or both up- and downward reserve requirements. In particular, the optimal BESS sizing from the only upward reserve requirement scenario shows the higher discrepancy with 14.3 MW compared to the 8.1 and 6.3 MW from the only downward reserve and both up- and downward reserve scenarios respectively, i.e., 77 % and 126 % difference. Overall, results from scenarios with only downward reserve requirements align more closely with the up- and downward reserve scenarios than with the only upward reserve scenario, especially when FFGs are the sole providers of reserves with a maximum divergence of around 30 % for the optimal BESS. Conversely, the integration of BESS for reserve provision brings all scenarios closer to the BS, allowing for a considerable reduction in costs and enabling greater penetration of vRES. In other words, the BESS can supply reserves in a way that mitigates the constraints on reserve requirements, aligning the techno-economic optimization with the results seen in the BS, with higher difference for the optimal sizing for the BESS technology of 16.4 MW for the up reserve scenario compared to 15.2 MW for the BS. Moreover, when BESS provides reserve capacity, both the only upward reserve and only downward reserve scenarios fall within a 5 % margin of difference from the up-and downward reserve scenario.

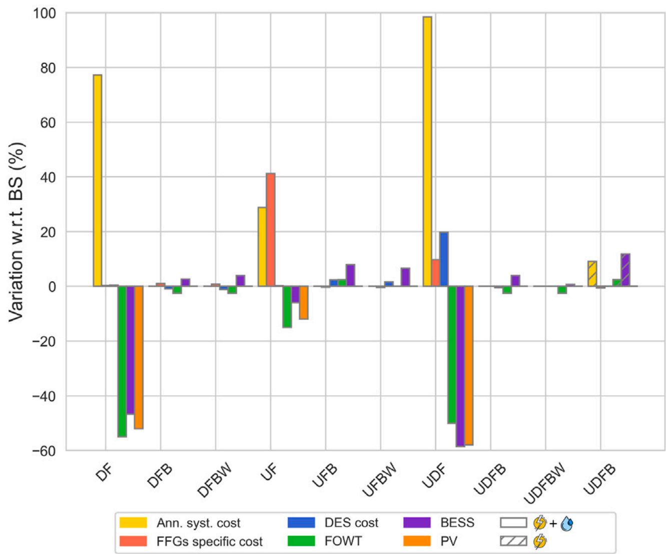

Fig. 4. Technology sizing and costs of the FF scenarios relative to the base scenario (BS).

Fig. 5 shows the distribution of load factors across different operational hours for each FFG and DES unit under scenarios with only downward reserve, only up- reserve and both up- and downward reserve requirements. The figure includes cases where only FFGs provide reserves (first row) and cases where both FFGs and BESS can provide power reserves (second row), providing insights into why downward reserve requirements are more restrictive than upward reserve requirements. Therefore, when only FFGs provide flexibility, in scenarios with only upward reserve requirements, the system finds an economic optimum by operating FFGs at their minimum load (resulting in a higher specific cost equal to 708 €/MWh compared to 498 €/MWh of the BS- see Fig. 4) favoring vRES penetration, which is overall more cost-effective. In these cases, the optimizer chooses to keep the generator online but operating significantly below the maximum level required to guarantee upward reserve. Referring to the scenario with only downward reserve requirements, the optimal techno-economic solution tends to minimize production from FFGs in favor of increased penetration of vRES, as evidenced by lower fuel costs and objective function values. Yet, with downward reserve constraints, generators are forced to increase the actual power output with respect to scenario with only upward reserve requirements, reducing the specific cost of diesel, which is equal to 503.0 €/MWh compared to 708 €/MWh of the only up reserve scenario, due to the amortization of standby costs but increasing the overall system cost, resulting in an objective function equal to 11.74 M €compared to 8.47 M €of the only up reserve scenario. This is because, in the absence of downward reserve requirements, the system would ideally produce less from FFGs, even at a higher specific cost, to favor greater renewable penetration. Consequently, the energy planning for the downward reserve-only scenario more closely resembles the up- and downward reserve scenario than the upward reserve-only scenario. Overall, in upward reserve-only scenarios, generators operate at a higher specific cost but achieve a lower objective function equal to 8.47 M €, compared to downward -reserve and up- and downward reserve cases where it is equal to 11.74 M €and 13.13 M €respectively, corresponding to a 39 % and 55 % increase in system costs. The system prefers not to fully exploit the generator's capacity, allowing for greater vRES penetration equal to 80.1 %, compared to 37 % and 32.5 % for only down reserve and up- and downward reserve scenarios respectively. However, when BESS is allowed to provide reserves, the outcomes align consistently across different reserve requirement scenarios, both in terms of costs and operational load factor distributions. Furthermore, in scenarios

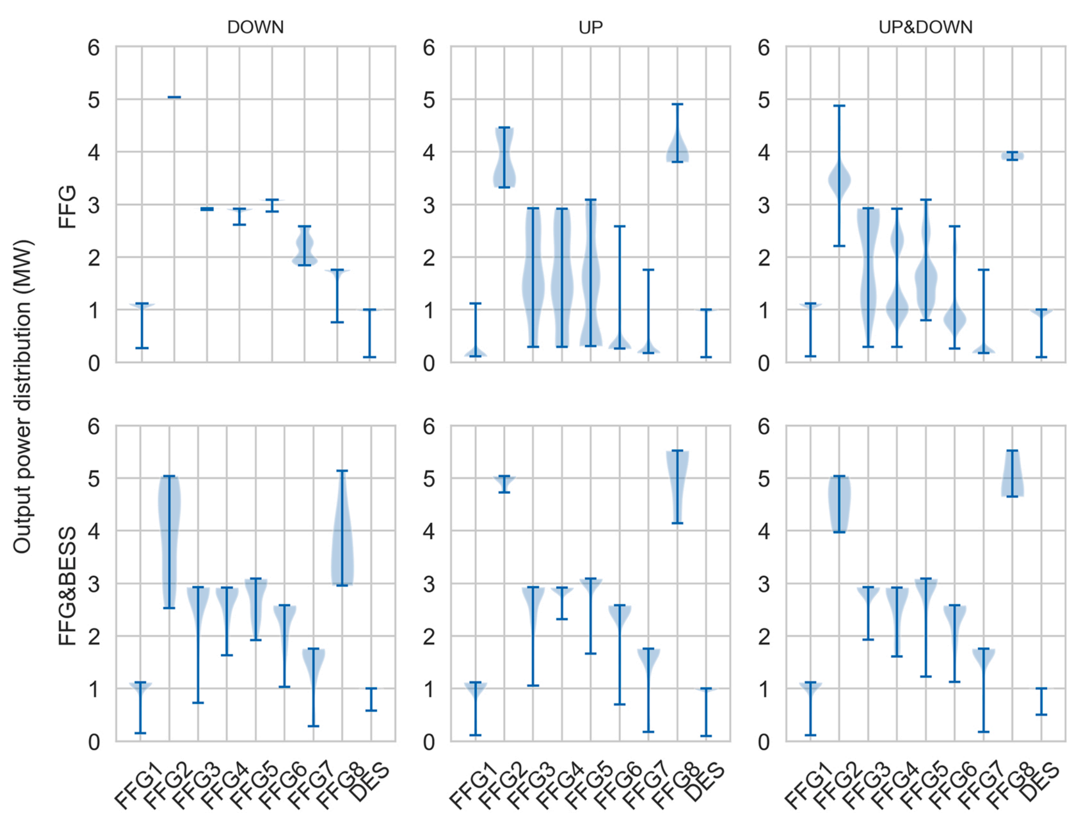

Fig. 5. Distribution of load factor across operational hours for FFGs and DES in FF scenarios.

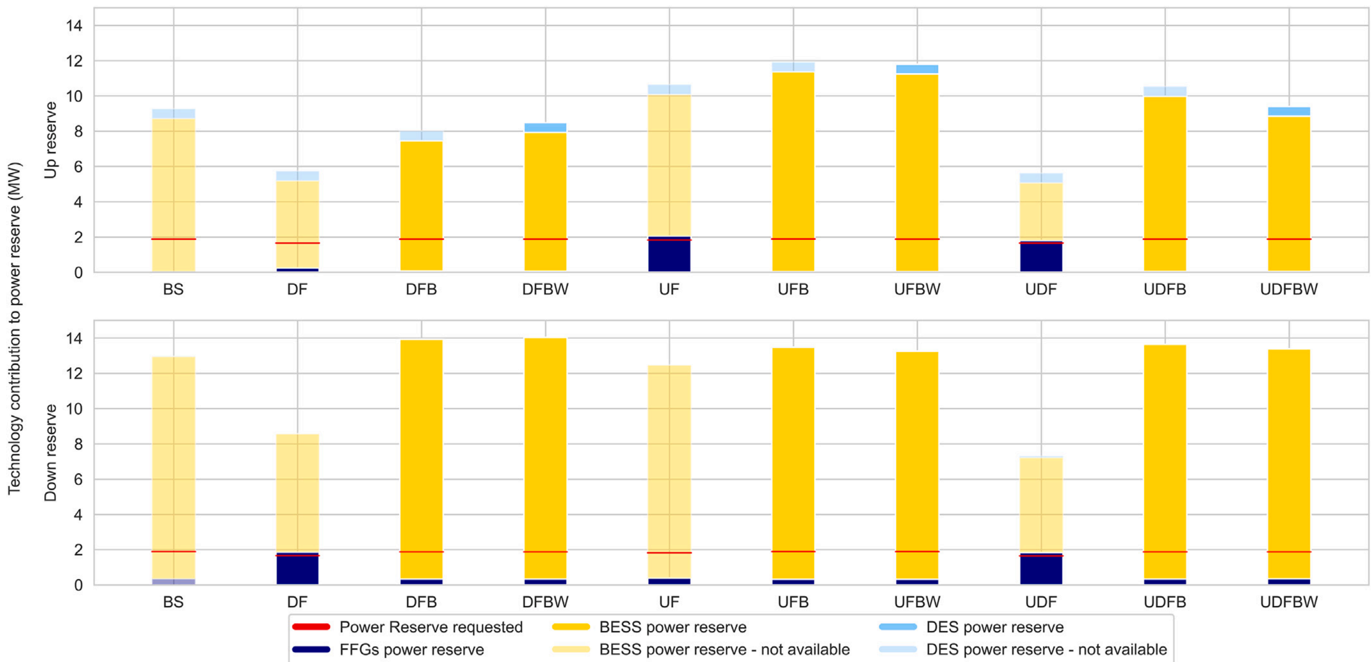

Fig. 6. Technology contribution to power reserve reqs. in FF scenarios.

where BESS can provide reserves, the diesel generators operate significantly fewer hours, with a maximum of 272 working hours for the up- and downward reserve scenario with respect to 2482 h of the BS, and, when active, generally at their maximum load factor, resulting in lower specific fuel costs, with a maximum of 506.8 €/MWh for the only down reserve scenario, and overall fuel consumption, with a maximum of 741 Ml of fuel for the up- and down reserve scenario compared to 1258.8 Ml of the BS. Under the assumption of 2.7 $kgCO_2e$ per liter of diesel fuel [52,53], this corresponds to a pass from approximately 2.0 to $3.3 \cdot 10^6$ tonnes of CO_2e per year.

Fig. 6 presents the mean annual hourly power reserve available for the different FF scenarios, broken down by the contribution from each technology. In the figure, dark colors represent the contribution to the power reserve requirements from technologies that are explicitly modeled in the MILP energy planning model. Conversely, transparent colors indicate the potential contributions from technologies when their contribution is not directly modeled in the MILP optimization (for example, the BESS contribution in UF scenarios). This unmodeled contribution is calculated in post-processing and represents a possible additional reserve that the MILP model does not consider during optimization. As a result, when a specific technology is not included in the reserve provision within the model, the reserve needs must be met by other available technologies. The figure shows how BESS reserves, even when not integrated into the model, could significantly contribute to the system's ability to meet reserve requirements. Indeed, as can be seen from the bar chart, the scenarios where FFGs are the only provider of reserve capacity show a huge contribution of the BESS to the reserve supply, i.e., in the only up and up and down reserve scenarios, the upward reserve contribution is equal to 8 MW and 3 MW respectively, with a corresponding upward reserve requirement of 1.82 MW and 1.65 MW respectively; while for the downside only and upside and downside scenarios, the downside reserve contribution from BESS is 6.7 MW and 5.4 MW respectively, with a corresponding downside reserve requirement of 1.65 MW in both scenarios. In scenarios where BESS can provide reserves, the FFGs' contribution to reserve is nearly null. In fact, in these scenario configurations, where both FFGs and BESS can contribute to the power reserve supply, the FFGs and BESS contributions are 0.03 MW and 11.3 MW respectively for the up-only reserve scenario, and 0.04 MW and 10 MW for the upward reserve demand and 0.34 MW and 13.3 MW for the downward reserve demand respectively, for the up and down scenarios. In the only scenario with down reserves, the reserve supply of FFGs is 0.34 MW, while the BESS is 14 MW. In these scenarios, FFGs tend to operate in a more binary, on-off manner (see Fig. 5), allowing them to run at peak efficiency while BESS fulfills the reserve requirements. Considering the hourly analysis of the different scenarios, the BESS is able to satisfy the reserve requirement when configured as possible reserve supplier for at least the 85 % of the total hours simulated, and besides when it is also not considered as possible reserve provider for at least 63 % of the total hours it is able to satisfy the reserve demand. This result underscores the importance of incorporating BESS reserve capabilities directly into the long-term dispatch analysis, as well as accurately modeling the costs associated with FFGs and reserve provisions.

Fig. 7 presents the distribution of the hourly surplus (relative to the reserve requirements) of available reserves across the different scenarios, sorted in descending order. In Fig. 7a, the available reserve is calculated by including the contributions from all technologies, regardless of whether they are modeled in each specific scenario. Conversely, in Fig. 7b, the available reserve is computed based on the modeled contributions for each scenario (i.e., in the UF scenario, only the contribution from FFGs is considered). The plots confirm that BESS, even when not explicitly modeled in the MILP, would be capable of meeting reserve requirements for nearly 70 % of the simulated hours. Fig. 7a further emphasizes the potential impact of BESS in reserve provision, highlighting the importance of modeling its role. Additionally, constraints on upward reserves seem more challenging from a reserve requirement perspective: DF scenario consistently meets upward reserve requirements for almost 70 % of the simulated hours, while scenarios with UF meet downward reserve requirements for nearly 95 % of the simulated hours. Yet, this is only true if we include the role of BESS in power reserve supply, even when the MILP energy planning is not informed about its role. Overall, the DF scenario yields results more closely aligned with the UDF scenario than with DF, suggesting that downward reserve requirements should not be neglected when BESS cannot provide reserves. Fig. 7 emphasizes the importance of incorporating upward reserve demands as well.

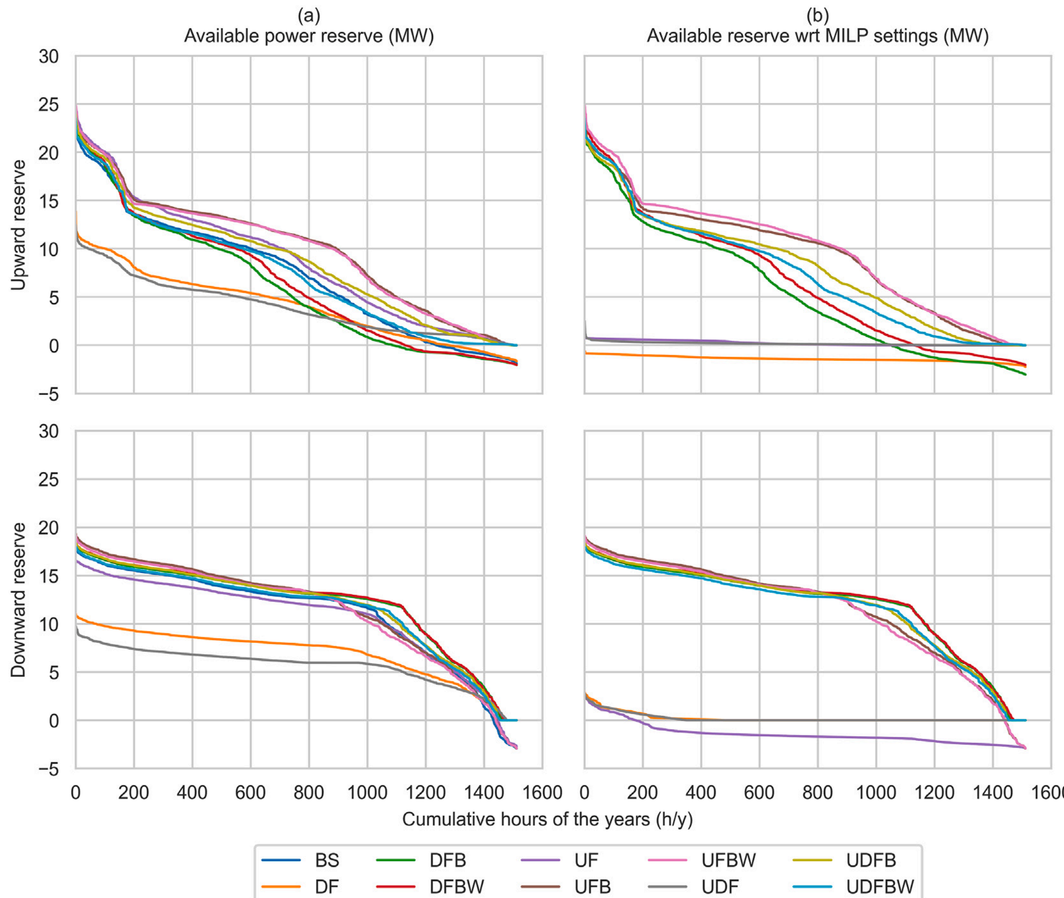

Fig. 7. Surplus reserve distributions across scenarios: (a) considering all available technologies, (b) based on the specific configuration of each scenario.

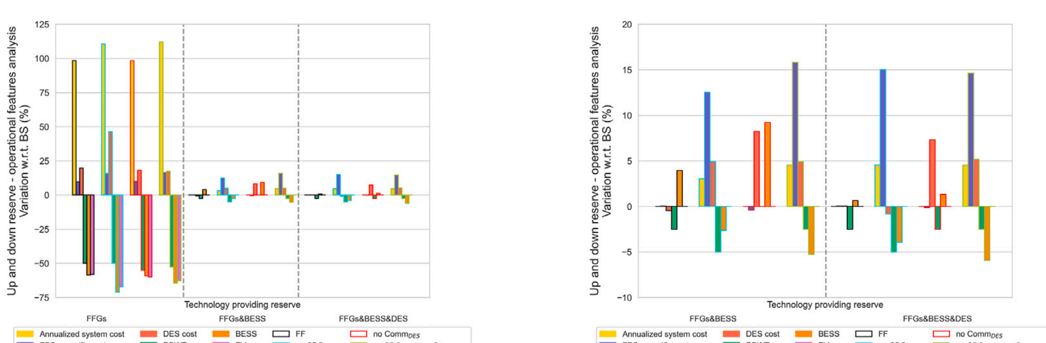

(a) All scenarios. (b) BESS reserve scenarios.

Fig. 8. Comparison of technology sizing and costs with and without operational constraints.

5.3. Integrating water demand into the energy system: fixed electrical load vs. sector coupling

This section examines the impact of integrating freshwater demand into the energy planning model by comparing scenarios with a fixed electrical load for water production to those allowing flexible scheduling of desalination operations. As shown in Fig. 4, scenarios with a fixed water production load increase the system's BESS capacity requirements from 15.8 MW to 17 MW, as the model must accommodate a higher baseline electrical demand. In contrast, when desalination schedules are flexible, the system can determine the timing of freshwater production to align with periods of high renewable generation, thereby meeting the same total water demand over time. This flexibility reduces the reliance on BESS by shifting desalination operations to coincide with renewable energy availability, reducing the required BESS capacity and ultimately lowering system costs, from 7.24 M €to 6.61 M €(−10 %), while also enabling greater integration of vRES, from 86.5 % to 88.5 %. In addition, this shift leads to a 26.5 % reduction in diesel fuel consumption, as the system leverages the flexibility of desalination to align load with vRES availability rather than relying on fossil-based generation. This form of sector coupling not only improves operational flexibility, but also supports the structural decarbonization of isolated energy systems by reducing storage needs, cutting fuel consumption, and increasing vRES integration. These benefits could become even more critical in future

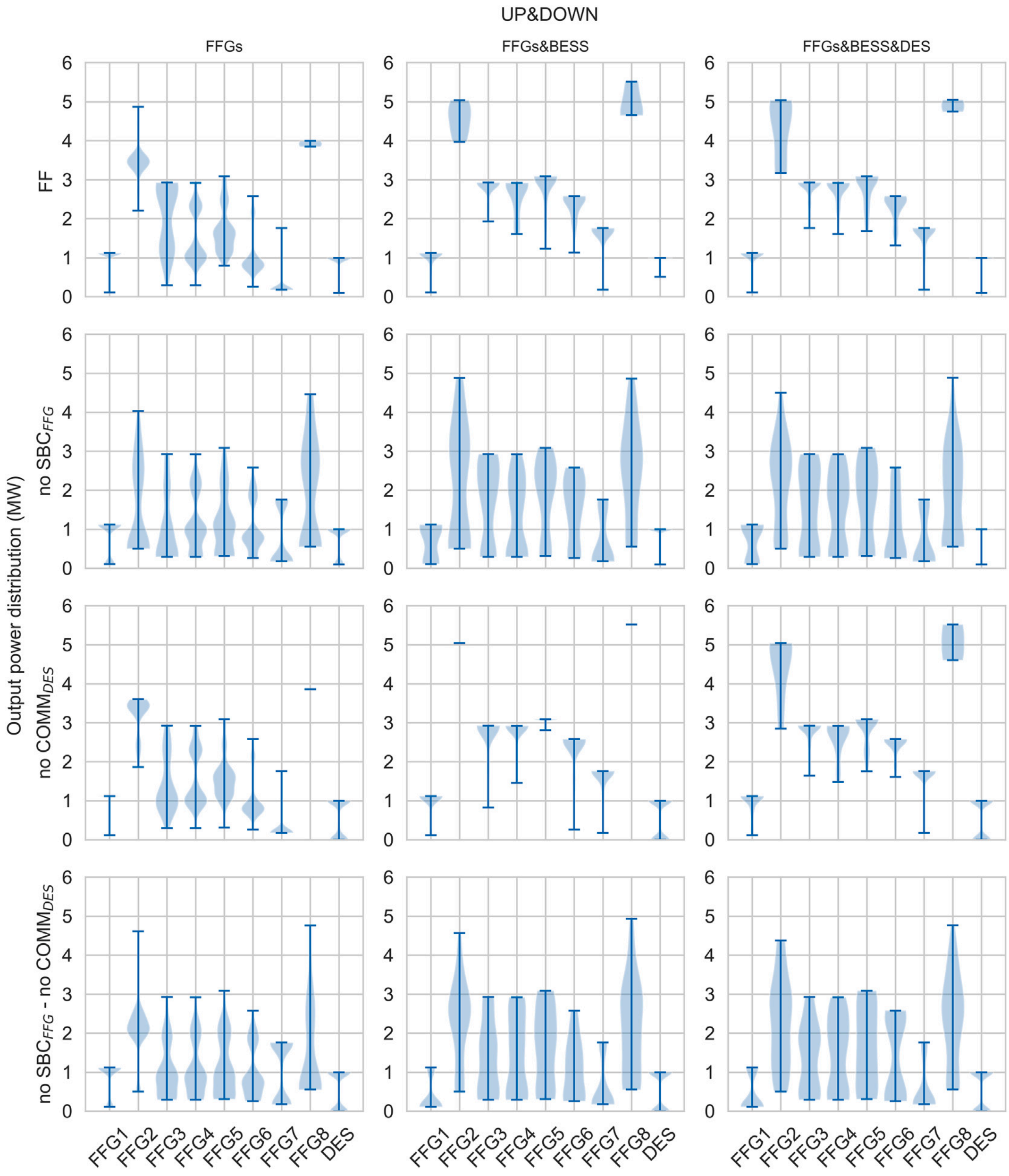

Fig. 9. FFG load factor distribution across scenarios.

scenarios where climate change exacerbates freshwater scarcity, potentially increasing reliance on desalination and further strengthening the role of water-energy co-optimization [54,55].

5.4. Operational features impact on energy planning

Figs. 8–10 illustrate the impact of including standby costs (SBC) for FFGs and specific operational constraints for DES on the energy planning model, as well as on the load distribution across FFGs and DES.

Fig. 8 compares the optimal nominal capacities for PV, FOWT, and BESS along with the annualized system costs and marginal costs associated with FFGs under different operational settings (removing SBC for FFGs, removing commitability for DES, and both) relative to the baseline scenario (FF). Results indicate that incorporating SBC for FFGs (sbc_{FFG}) has minimal influence on overall system costs, with a maximum deviation of less than 6 % for the up- and down reserve scenario with and without SBC for the FFGs as only technology providing reserve. On optimal energy planning side, more critical differences can be noted for the BESS optimal size which differs by the around 40 % for the up- and down reserve scenario not considering FFGs' SBC with respect to the comprehensive one. Regarding the operational side, desalinator costs differ by the around the 22 % with 190 k €for the up- and down reserve scenario with SBC, compared to 232 k €for the corresponding scenario without SBC. The optimal capacities for each technology remain relatively stable across scenarios, highlighting the limited macro-level impact of sbc_{FFG} on energy planning. However, Fig. 9 reveals that SBC affects operational behavior by pushing FFGs toward higher load factors. Specifically, in scenarios with SBC, the system tends to maintain higher FFG load factors to avoid standby penalties. This effect is more pronounced in scenarios with multiple reserve requirements, such as UDFB and UDFBW, where the system strategically minimizes standby losses. The UDF scenario exhibits a milder shift, though a trend toward higher load factors persists across configurations, underscoring how SBC encourages FFGs to operate near optimal load levels to mitigate cost implications. It should be noted, however, that frequent cycling may in practice accelerate

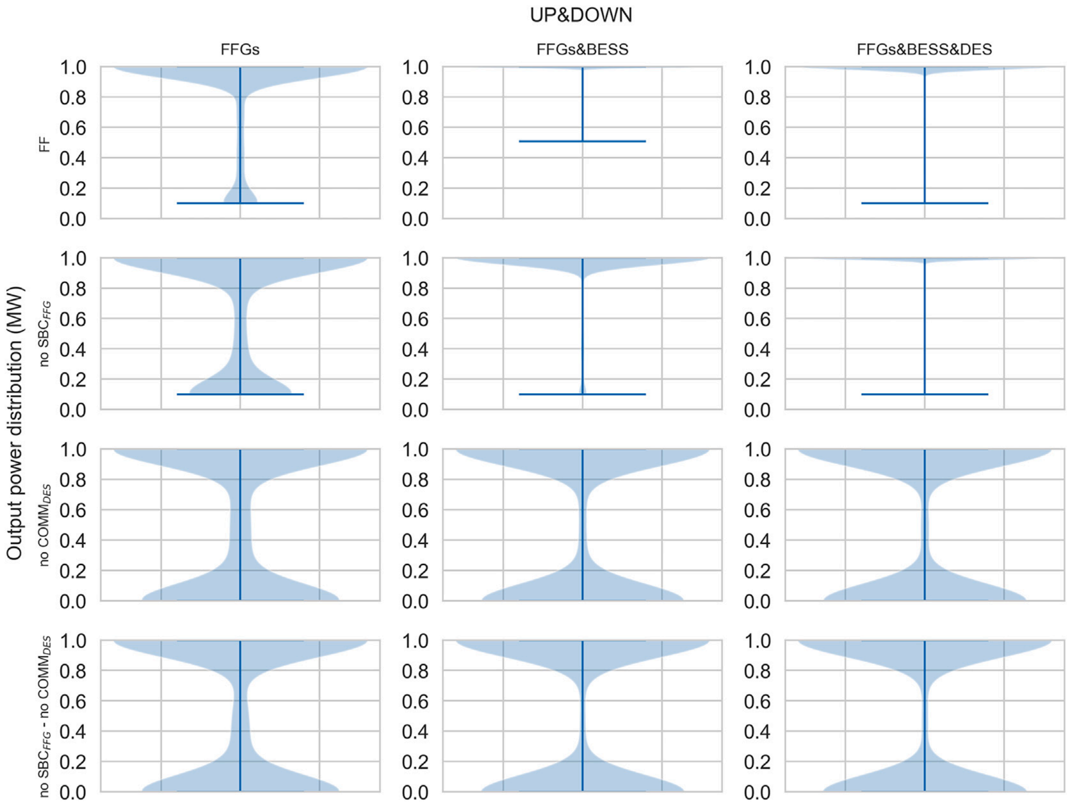

Fig. 10. DES load distribution across scenarios.

wear and increase O&M requirements, even though such effects are not explicitly modeled here.

As shown in Fig. 8b, which focuses on the reserve cases where the BESS technology can provide reserve capacity, removing DES commitability constraints impacts BESS's role, leading to an overestimation in optimal BESS capacity when BESS can provide reserve, as observed with a +6 % increase relative to the FF case. However, the load factor distribution for FFGs does not significantly change with the removal of DES commitability. Scenarios where both FFG SBC and DES commitability are neglected align closely with scenarios where only SBC is omitted, in terms of both technology sizing and load distribution among generators.

Finally, Fig. 10 provides insights into the load distribution of DES across scenarios, highlighting that: 1) neglecting SBC for FFGs increases DES usage at lower loads, especially when only FFGs can provide reserves; and 2) DES operational constraints significantly influence DES's working load distribution even when BESS can provide reserves. Although DES operational aspects strongly affect its working conditions, DES has a limited role in overall outcomes, primarily due to the specific characteristics of the case study. In scenarios where water production demand increases, DES operational features will likely play a more critical role in the system's behavior.

6. Conclusions

This study presents a comprehensive planning framework for non-interconnected islands, systematically evaluating the combined effects of reserve requirements, flexible DES operations, and detailed operational constraints of FFGs and BESS. By progressively adding these features, the study provides a robust analysis of their individual and synergistic impacts on system optimization.

The results demonstrate that incorporating both upward and downward reserve requirements leads to significantly different system configurations. In particular, scenarios with both reserves show a 40 % increase in optimal BESS capacity and a 55 % increase in total system cost compared to configurations with only upward reserves. Additionally, BESS integration improves system flexibility, reducing the specific fuel consumption of FFGs by 20 % and lowering overall emissions and operational costs.

The integration of flexible desalination operations proved to be equally transformative. By aligning water production with periods of high renewable generation, the system reduced reliance on storage, mitigated renewable curtailment, and improved resource efficiency. Flexible desalination alone resulted in a 10 % reduction in annual system costs, primarily due to the lower BESS capacity required and a 26.5 % decrease in diesel fuel consumption, as the system relies more on vRES. These findings underscore that integrating water systems can accelerate the energy transition by reducing costs while maximizing renewable energy utilization, with vRES penetration reaching 88.5 % in optimized scenarios. These findings emphasize that integrating water systems can accelerate the energy transition by reducing costs while maximizing renewable energy utilization, even under current economic conditions and without accounting for carbon pricing.

The study also highlights the critical role of accurately modeling operational constraints through unit commitment. This includes factors such as the minimum working rate and standby costs for FFGs, as well as the minimum uptime, minimum working rate, and standby costs for DESs. Scenarios that neglect these constraints overestimate system costs and fuel consumption, demonstrating the necessity of realistic operational models to support informed decision making. Similarly, the operational flexibility of DES was shown to play a vital role in providing reserves and optimizing load distribution.

While the present work provides a robust and operationally detailed planning framework, future research could build on this foundation by investigating the sensitivity of results to key techno-economic assumptions—such as renewable investment costs, BESS degradation rates, or reserve requirements—as well as to different system characteristics, including renewable mixes and heterogeneous load profiles, thus further assessing system resilience under uncertainty.

Overall, this work establishes that a holistic approach to energy and water system planning is vital for the sustainable transition of isolated power systems. By addressing the interplay between reserve requirements, operational constraints, and sector coupling, the study offers a clear pathway toward achieving energy self-sufficiency and decarbonization, setting a new benchmark for optimizing energy systems in non-interconnected islands.

CRediT authorship contribution statement

Enrico Giglio: Writing – review & editing, Writing – original draft, Software, Methodology, Investigation, Data curation, Conceptualization. **Caterina Carà:** Writing – original draft, Data curation. **Edoardo Pasta:** Writing – review & editing, Writing – original draft. **Edoardo Destro:** Writing – original draft, Software, Methodology, Investigation, Data curation. **Anna Ceni:** Writing – original draft. **Giovanni Bracco:** Writing – review & editing, Supervision, Project administration. **Giuliana Mattiazzo:** Writing – review & editing, Supervision, Project administration, Funding acquisition.

Declaration of competing interest

The authors declare that they have no known competing financial interests or personal relationships that could have appeared to influence the work reported in this paper.

Acknowledgements and funding

The Project is funded under the National Recovery and Resilience Plan (NRRP), Italy, Mission 4 Component 2 Investment 1.3 - Call for tender No. 1561 of 11.10.2022 of Ministero dell' Università e della Ricerca (MUR); funded by the European Union – NextGenerationEU Award Number: Project code PE0000021, Concession Decree No. 1561 of 11.10.2022 adopted by Ministero dell'Università e della Ricerca (MUR), Italy, CUP, Italy E13C22001890001, Project title "Network 4 Energy Sustainable Transition – NEST". This work was supported by the Politecnico di Torino through the CRUI CARE Agreement.

Appendix A. Scenario settings

See Table A.3.

Table A.3
The different scenarios are identified by specific acronyms: FF stands for Full Features, FFGs-OF stands for FFGs Operational Features, WD-OF stands for Water Demand Operational Features, WD-ED stands for Water Demand as Electricity Demand.

Scenarios		FFGs		Water system integration				Power reserve model				
		p_g^{min}	sbc_g	p_d^{min}	sbc_d	T_d^{mu}	WD coupling?	Rrq	Qrq	reserve provider		
										FFG	BESS	DES
FF	BS	X	X	X	X	X	X					
	DF	X	X	X	X	X	X		X	X		
	DFB	X	X	X	X	X	X		X	X	X	
	DFBW	X	X	X	X	X	X		X	X	X	
	UF	X	X	X	X	X	X	X		X		
	UFB	X	X	X	X	X	X	X		X	X	
	UFBW	X	X	X	X	X	X	X		X	X	X
	UDF	X	X	X	X	X	X	X	X	X		
	UDFB	X	X	X	X	X	X	X	X	X	X	
	UDFBW	X	X	X	X	X	X	X	X	X	X	X
FFG-OF	UDF	X		X	X	X	X	X	X	X		
	UDFB	X		X	X	X	X	X	X	X	X	
	UDFBW	X		X	X	X	X	X	X	X	X	X
WD-OF	UDF	X	X				X	X	X	X		
	UDFB	X	X				X	X	X	X	X	
	UDFBW	X	X				X	X	X	X	X	X
OF	UDF	X					X	X	X	X		
	UDFB	X					X	X	X	X	X	
	UDFBW	X					X	X	X	X	X	X
WD-ED	UDFB	X	X	n.a.	n.a.	n.a.		X	X	X	X	

Appendix B. Scenario results

See Table B.4.

Table B.4
Optimization results of the different scenarios classified with respect to the specific operational features implemented.

Case study		Time	Comp.	MIP	f_{obj}	f^{*}_{obj}	PV	FOWT	BESS		RES	Work. hr	Avg. FFGs	Max FFGs	Fuel	OC_F	oc_F	OC_D
		hor.	time (s)	Gap (%)	(M€)	(M€)	(MW)	(MW)	(MWh)	(MW)	(%)	FFGs (h)	on (#/h)	on (#/h)	(kl)	(M€)	(€/MWh)	(k€)
FF	BS	FY	213	1.2	7.56	7.56	15	3.8	28.9	14.4	82	2482	0.3	4	1258.8	2.85	497.6	155
	DFBW	FY	1811	1.0	7.57	7.57	15	3.9	29.1	14.6	82.3	2716	0.3	4	1237.5	2.80	497.5	155
	UFBW	FY	512	0.8	7.56	7.56	15	3.8	28.1	14	81.7	3428	0.4	4	1281.3	2.91	499.0	158
	UDFBW	FY	810	0.9	7.59	7.59	15	3.8	28.6	14.3	81.8	2884	0.3	4	1277.2	2.90	499.2	156
	BS	TW	35	1.0	6.56	6.56	15	4	30.4	15.2	88.3	332	0.2	3	748	1.71	501.7	159
	DF	TW	1586	2.0	11.74	11.74	7.2	1.8	16.3	8.1	37	1580	1	2	4044.7	9.24	503.0	159
	DFB	TW	68	1.9	6.6	6.6	15	3.9	31.2	15.6	88.4	248	0.2	2	744.3	1.71	506.8	157
	DFBW	TW	56	1.9	6.6	6.6	15	3.9	31.5	15.8	88.5	235	0.2	2	736.9	1.69	505.7	157
	UF	TW	3531	3.0	8.47	8.47	13.2	3.4	28.5	14.3	80.1	1863	1.2	3	1356.2	4.11	708.2	159
	UFB	TW	15	2.0	6.62	6.62	15	4.1	32.9	16.4	89.1	245	0.2	2	697.1	1.59	500.4	162
	UFBW	TW	16	1.8	6.6	6.6	15	4	32.4	16.2	88.8	270	0.2	2	716.5	1.63	499.9	161
	UDF	TW	100,895	1.7	13.13	13.13	6.3	2	12.6	6.3	32.5	2919	1.9	3	4393.4	10.83	550.4	190
	UDFB	TW	166	1.1	6.61	6.61	15	3.9	31.5	15.8	88.5	272	0.2	3	741	1.69	501.9	158
	UDFBW	TW	35	0.8	6.59	6.59	15	3.9	30.7	15.3	88.2	288	0.2	2	756.7	1.73	502.0	158
FFGs-OF	UDF	TW	2618	2.0	10.71	13.87	4.9	2	8.8	4.4	30	3462	2.3	7	4601.1	11.86	580.4	232
	UDFB	TW	11	1.0	6.33	6.84	15	3.8	29.6	14.8	87.5	358	0.2	4	815.2	2.05	564.6	166
	UDFBW	TW	12	0.8	6.32	6.88	15	3.8	29.3	14.6	87.3	425	0.3	4	835.3	2.14	577.1	157
WD-OF	UDF	TW	3722	1.9	12.96	13.14	6	1.8	12.4	6.2	31.9	2842	1.9	3	4436.3	10.95	551.4	187
	UDFB	TW	19	1.8	6.47	6.64	15	4	33.2	16.6	89.2	256	0.2	2	693.1	1.57	499.8	171
	UDFBW	TW	68	0.9	6.43	6.6	15	3.9	30.8	15.4	88.3	287	0.2	2	752.4	1.71	501.1	170
OF	UDF	TW	707	1.8	10.54	13.95	5.6	1.9	10.7	5.4	30.4	2804	1.9	7	4579.1	11.88	584.9	186
	UDFB	TW	8	0.5	6.16	6.9	15	3.9	28.8	14.4	87.3	458	0.3	4	832.1	2.15	581.1	166
	UDFBW	TW	8	0.2	6.15	6.86	15	3.9	28.7	14.3	87.3	462	0.3	3	832.3	2.13	575.1	167
WD-EL	UDFB	FY	350	0.9	8.04	8.05	15	3.8	33.8	16.9	82.5	3854	0.4	4	1413.9	3.21	499.2	n.a.
	UDFB	TW	104	0.9	7.24	7.24	15	4.1	33.9	17	86.5	326	0.2	2	1008	2.29	499.0	n.a.

Data availability

Data are sourced from public databases cited in the manuscript. The optimization model is implemented in open-source code to ensure transparency and replicability.

References

[1] International Energy Agency. Renewables 2024. Analysis and forecast to 20230. OECD Publishing; 2024. https://www.iea.org/reports/renewables-2024

[2] IRENA. Planning for the renewable future: long-term modelling and tools to expand variable renewable power in emerging economies, Tech. rep., International Renewable Energy Agency; 2017 Dec.

[3] IRENA. Transforming small-island power systems: technical planning studies for the integration of variable renewables, Tech. rep., International Renewable Energy Agency; 2018 Dec.

[4] Mimica M, Krajačić G. The smart islands method for defining energy planning scenarios on islands. Energy 2021;237:121653. https://doi.org/10.1016/j.energy.2021.121653. https://www.sciencedirect.com/science/article/pii/S0360544221019010

[5] Alves M, Segurado R, Costa M. On the road to 100% renewable energy systems in isolated islands. Energy 2020;198:117321. https://doi.org/10.1016/j.energy.2020.117321. https://www.sciencedirect.com/science/article/pii/S036054422030428X

[6] Mehrjerdi H. Modeling and optimization of an island water-energy nexus powered by a hybrid solar-wind renewable system. Energy 2020;197:117217. https://doi.org/10.1016/j.energy.2020.117217. https://www.sciencedirect.com/science/article/pii/S0360544220303248

[7] Tsai Y-C, Chiu C-P, Ko F-K, Chen T-C, Yang J-T. Desalination plants and renewables combined to solve power and water issues. Energy 2016;113:1018–30. https://doi.org/10.1016/j.energy.2016.07.135. https://www.sciencedirect.com/science/article/pii/S0360544216310593

[8] Dranka GG, Ferreira P, Vaz AIF. A review of co-optimization approaches for operational and planning problems in the energy sector. Appl Energy 2021;304:117703. https://doi.org/10.1016/j.apenergy.2021.117703. https://www.sciencedirect.com/science/article/pii/S0306261921010588

[9] IRENA. Electricity storage and renewables: costs and markets to 2030, Tech. rep., International Renewable Energy Agency; 2017 Dec.

[10] Hu Y, Armada M, Jesús Sánchez M. Potential utilization of battery energy storage systems (BESS) in the major European electricity markets. Appl Energy 2022;322:119512. https://doi.org/10.1016/j.apenergy.2022.119512. https://www.sciencedirect.com/science/article/pii/S0306261922008340

[11] Branco H, Castro R, Setas Lopes A. Battery energy storage systems as a way to integrate renewable energy in small isolated power systems. Energy Sustain Dev 2018;43:90–9. https://doi.org/10.1016/j.esd.2018.01.003. https://www.sciencedirect.com/science/article/pii/S0973082617311675

[12] Hamdi M, El Salmawy HA, Ragab R. Incorporating operational constraints into long-term energy planning: the case of the Egyptian power system under high share of renewables. Energy 2024;300:131619. https://doi.org/10.1016/j.energy.2024.131619. https://www.sciencedirect.com/science/article/pii/S0360544224013926

[13] Wyrwa A, Suwała W, Pluta M, Raczyński M, Zyśk J, Tokarski S. A new approach for coupling the short- and long-term planning models to design a pathway to carbon neutrality in a coal-based power system. Energy 2022;239:122438. https://doi.org/10.1016/j.energy.2021.122438. https://www.sciencedirect.com/science/article/pii/S0360544221026876

[14] Cuisinier E, Lemaire P, Ruby A, Bourasseau C, Penz B. Impact of operational modelling choices on techno-economic modelling of local energy systems. Energy 2023;276:127599. https://doi.org/10.1016/j.energy.2023.127599. https://www.sciencedirect.com/science/article/pii/S0360544223009933

[15] Groppi D, Feijoo F, Pfeifer A, Garcia DA, Duic N. Analyzing the impact of demand response and reserves in islands energy planning. Energy 2023;278:127716.

[16] Curto D, Favuzza S, Franzitta V, Guercio A, Navia MAN, Telaretti E, et al. Grid stability improvement using synthetic inertia by battery energy storage systems in small islands. Energy 2022;254:124456.

[17] Psarros GN, Nanou SI, Papaefthymiou SV, Papathanassiou SA. Generation scheduling in non-interconnected islands with high RES penetration. Renew Energy 2018;115:338–52.

[18] Gacitúa L, Olivares D, Negrete-Pincetic M, Lorca Á. The role of fast-acting energy storage for contingency grid support in the transmission planning. Energy 2023;283:128465. https://doi.org/10.1016/j.energy.2023.128465. https://www.sciencedirect.com/science/article/pii/S0360544223018595

[19] Singh B, Kumar A. Optimal energy management and feasibility analysis of hybrid renewable energy sources with BESS and impact of electric vehicle load with demand response program. Energy 2023;278:127867. https://doi.org/10.1016/j.energy.2023.127867. https://www.sciencedirect.com/science/article/pii/S0360544223012616

[20] Bahloul M, Daoud M, Khadem SK. Optimal dispatch of battery energy storage for multi-service provision in a collocated PV power plant considering battery ageing. Energy 2024;293:130744. https://doi.org/10.1016/j.energy.2024.130744. https://www.sciencedirect.com/science/article/pii/S0360544224005164

[21] Mentis D, Karalis G, Zervos A, Howells M, Taliotis C, Bazilian M, et al. Desalination using renewable energy sources on the arid islands of South Aegean Sea. Energy 2016;94:262–72.

[22] Meerganz von Medeazza G, Moreau V. Modelling of water–energy systems. The case of desalination. Energy 2007;32(6):1024–31, third Dubrovnik conference on sustainable development of energy, water and environment systems. https://doi.org/10.1016/j.energy.2006.10.006. https://www.sciencedirect.com/science/article/pii/S0360544206002726

[23] Segurado R, Krajačić G, Duić N, Alves L. Increasing the penetration of renewable energy resources in S. Vicente, Cape Verde. Appl Energy 2011;88(2):466–72.

[24] Cabrera P, Folley M, Carta JA. Design and performance simulation comparison of a wave energy-powered and wind-powered modular desalination system. Desalination 2021;514:115173. https://doi.org/10.1016/j.desal.2021.115173. https://www.sciencedirect.com/science/article/pii/S0011916421002447

[25] Corsini A, Rispoli F, Gamberale M, Tortora E. Assessment of H2-and H2O-based renewable energy-buffering systems in minor islands. Renew Energy 2009;34(1):279–88.

[26] Groppi D, Nastasi B, Prina MG, Astiaso Garcia D. The eplanopt model for Favignana Island's energy transition. Energy Convers Manag 2021;241:114295. https://doi.org/10.1016/j.enconman.2021.114295. https://www.sciencedirect.com/science/article/pii/S0196890421004714

[27] Massaro F, Pace G, Sanseverino ER, Tanaka K, Zizzo G. An algorithm for optimal sizing of BESS in smart islands energy communities: the case of Pantelleria. In: 2021 IEEE international conference on environment and electrical engineering and 2021 IEEE industrial and commercial power systems Europe (EEEICI&CPS Europe); 2021. p. 1–6. https://doi.org/10.1109/EEEIC/ICPSEurope51590.2021.9584620

[28] Borretta E, Giglio E, Luzzani G, Terranova V, Trivigno G, Niccolai A, et al. Software-based solutions for the optimization of a building electric bill using integrated PV and storage systems: a case study. In: 2021 IEEE international conference on environment and electrical engineering and 2021 IEEE industrial and commercial power systems Europe (EEEICI&CPS Europe); 2021. p. 1–6. https://doi.org/10.1109/EEEIC/ICPSEurope51590.2021.9584626

[29] Martínez-Barbeito M, Gomila D, Colet P. Dynamical model for power grid frequency fluctuations: application to islands with high penetration of wind generation. IEEE Trans Sustain Energy 2023;14(3):1436–45.

[30] De Vos K, Petoussis AG, Driesen J, Belmans R. Revision of reserve requirements following wind power integration in island power systems. Renew Energy 2013;50:268–79.

[31] Giglio E, Fioriti D, Chihota MJ, Poli D, Bekker B, Mattiazzo G. Integrated stochastic reserve estimation and MILP energy planning for high renewable penetration: application to 2050 South African energy system. Sustain Energy Grids Netw 2025;42:101650. https://doi.org/10.1016/j.segan.2025.101650. https://www.sciencedirect.com/science/article/pii/S2352467725000323

[32] Brijs T, van Stiphout A, Siddiqui S, Belmans R. Evaluating the role of electricity storage by considering short-term operation in long-term planning. Sustain Energy Grids Netw 2017;10:104–17. https://doi.org/10.1016/j.segan.2017.04.002. https://www.sciencedirect.com/science/article/pii/S2352467716301102

[33] Knezović K, Marinakis A, Evrenosoglu CY, Oudalov A. Role of grid and bulk storage in the integration of variable renewable energy resources: framework for optimal operation-driven multi-period infrastructure planning. Energy 2021;226:120378. https://doi.org/10.1016/j.energy.2021.120378. https://www.sciencedirect.com/science/article/pii/S0360544221006277

[34] Hansen CW, Papalexopoulos AD. Operational impact and cost analysis of increasing wind generation in the island of Crete. IEEE Syst J 2011;6(2):287–95.

[35] Nikolaidis P, Chatzis S, Poullikkas A. Optimal planning of electricity storage to minimize operating reserve requirements in an isolated island grid. Energy Syst 2020;11(4):1157–74.

[36] Giglio E, Novo R, Mattiazzo G, Fioriti D. Reserve provision in the optimal planning of off-grid power systems: impact of storage and renewable energy. IEEE Access 2023;11:100781–97. https://doi.org/10.1109/ACCESS.2023.3313979

[37] Giglio E, Edoardo P, Poli D, Mattiazzo G, Fioriti D. Capacity expansion and unit commitment with reserve requirements: a comparative analysis for an Italian off-grid island. In: 2025 21th international conference on the European energy market (EEM); 2025. p. 1–7.

[38] Critz DK, Busche S, Connors S. Power systems balancing with high penetration renewables: the potential of demand response in Hawaii. Energy Convers Manag 2013;76:609–19.

[39] Psarros GN, Kokkolios SP, Papathanassiou SA. Centrally managed storage facilities in small non-interconnected island systems. In: 2018 53rd international universities power engineering conference (UPEC); IEEE; 2018. p. 1–6.

[40] Prina MG, Groppi D, Nastasi B, Garcia DA. Bottom-up energy system models applied to sustainable islands. Renew Sustain Energy Rev 2021;152:111625.

[41] Oikonomou K, Parvania M. Optimal participation of water desalination plants in electricity demand response and regulation markets. IEEE Syst J 2019;14(3):3729–39.

[42] Groppi D, Kannan SKP, Gardumi F, Garcia DA. Optimal planning of energy and water systems of a small island with a hourly OSeMOSYS model. Energy Convers Manag 2023;276:116541.

[43] Amir Kavei F, Alfano ME, Quatraro F, Savoldi L. Integrated water-energy modeling in TEMOA energy system optimization model: Pantelleria case study.

[44] Brown T, Hörsch J, Schlachtberger D. PyPSA: Python for power system analysis. J Open Res Softw (2018).6(4). https://doi.org/10.5334/jors.188

[45] Zein A, Karaki S, Al-Hindi M. Analysis of variable reverse osmosis operation powered by solar energy. Renew Energy 2023;208:385–98. https://doi.org/10.1016/j.renene.2023.03.001. https://www.sciencedirect.com/science/article/pii/S0960148123002872

[46] Moscoloni C, Zarra F, Novo R, Giglio E, Vargiu A, Mutani G, et al. Wind turbines and rooftop photovoltaic technical potential assessment: application to Sicilian minor islands. Energies 2022;15(15):5548. https://doi.org/10.3390/en15155548. https://www.mdpi.com/1996-1073/15/15/5548

[47] Mehrjerdi H. Modeling and integration of water desalination units in thermal unit commitment considering energy and water storage. Desalination

2020;483:114411. https://doi.org/10.1016/j.desal.2020.114411. https://www.sciencedirect.com/science/article/pii/S0011916419323823

[48] Mohammadi F, Sahraei-Ardakani M, Al-Abdullah Y, Heydt GT. Can desalination be an economically viable solution for water scarcity? In: 2019 IEEE global humanitarian technology conference (GHTC); 2019. p. 1–4. https://doi.org/10.1109/GHTC46095.2019.9033050

[49] Airoldi D, Bertani D, Garofalo E, Guastella S, Lembo E, Sandroni C, et al. Scenari di sviluppo delle fer nelle isole minori italiane non interconnesse e analisi di casi studio, Tech. Rep. Rapporto 17004171, Ricerca sul Sistema Energetico – RSE S.p.A., Milano, Italy, deliverable n.14, as part of the Accordo di programma 2015-2017 with the Italian Ministry of Economic Development; (2017 Feb.)

[50] Fang Y, Han J, Du E, Jiang H, Fang Y, Zhang N, et al. Electric energy system planning considering chronological renewable generation variability and uncertainty. Appl Energy 2024;373:123961. https://doi.org/10.1016/j.apenergy.2024.123961. https://www.sciencedirect.com/science/article/pii/S0306261924013448

[51] Hoffmann M, Priesmann J, Nolting L, Praktiknjo A, Kotzur L, Stolten D. Typical periods or typical time steps? A multi-model analysis to determine the optimal temporal aggregation for energy system models. Appl Energy 2021;304:117825. https://doi.org/10.1016/j.apenergy.2021.117825. https://www.sciencedirect.com/science/article/pii/S0306261921011545

[52] Amakom CM, Ogungbenro OA, Iheonu NO, Nkwoada A, Iwueke DC, Anya J, et al. Annual carbon footprint from local electricity generation in federal University of Technology, Owerri, Imo State, Nigeria. Environ Health Insights 2022;16 https://doi.org/10.1177/11786302221136732

[53] Rozzi E, Giglio E, Moscoloni C, Novo R, Mattiazzo G, Lanzini A. Comparative study of electric and hydrogen mobility infrastructures for sustainable public transport: a PyPSA optimization for a remote island context. Int J Hydrogen Energy 2024;80:516–27. https://doi.org/10.1016/j.ijhydene.2024.07.105. https://www.sciencedirect.com/science/article/pii/S0360319924027769

[54] Corsini A, Tortora E. Sea-water desalination for load levelling of gen-sets in small off-grid islands. Energies 2018;11(8):2068. https://doi.org/10.3390/en11082068. https://www.mdpi.com/1996-1073/11/8/2068

[55] Pizzuti I, Magni GU, Delibra G, Garcia DA, Corsini A. Integrating desalination in renewable energy communities: a study on Ventotene Island. Renew Energy 2025;254:123759. https://doi.org/10.1016/j.renene.2025.123759. https://www.sciencedirect.com/science/article/pii/S0960148125014211